



ORIGINAL ARTICLES

2D-3D Modeling of Flow Over Sharp-Crested Weirs

Reda M. Abd El-Hady Rady

Researcher, Hydraulics Research Institute, National Water Research Center, Egypt.

ABSTRACT

The sharp-crested weir is the most commonly used device in channels for flow measurement and flow regulation due to its simplicity. Several attempts have been made to study in detail the flow over different shapes of normal conventional weirs including those with sharp crest, side weirs, and oblique weirs, mainly based on experimental work. On the contrary, little efforts have been done to use numerical models in investigating flow characteristics and pressure distribution over these types of weirs. The concern of this paper is to study flow over a rectangular sharp-crested weir and to provide a means of estimating its discharge coefficient. A 3D numerical model "Flow-3D" has been used for evolving a relationship to estimate the discharge coefficient for rectangular sharp-crested weirs. Several combinations of discharge and weir height have been employed to develop a best fit curve for estimating the discharge coefficients. The discharge coefficients estimated by the developed relationship has been found to be in good agreement with those listed in the literature well within a $\pm 3\%$ error. The study showed that the important variable governing discharge over sharp-crested weirs was H/t_w . Further, the advantages of "Flow -3D" as a tool for examining velocity vectors and pressure pattern over rectangular sharp-crested weirs have been highlighted.

Key words: Sharp-Crested weir; Volume of fluid method; Discharge coefficient.

Introduction

A weir is defined as an obstruction in an open channel that water must flow over and is used as an indirect method for obtaining the flow rate based on the weir geometry and head on the weir crest (King and Brater, 1963). The use of sharp-crested weirs in this research is to determine the flow characteristics and pressure distribution as well as to estimate discharge coefficient. The general weir equation for weirs with horizontal crests (King and Brater, 1963) is given in the following equation:

$$Q = C_d b h_w^{1.5} \quad (1)$$

In which, Q is the volumetric flow rate, h_w is the head on the weir crest, C_d is a weir discharge coefficient, and b is the length of the weir crest.

The discharge coefficient (C_d) depends on the effects of viscosity, the velocity distribution in the approach section, and capillarity, but it is most easily found by empirical methods (Rouse, 1950). This equation is useful in that one may determine the volumetric flow rate, Q , by simply measuring the head on the weir at an upstream location, assuming one has previously found the correct value of C_d for the weir being used.

Numerical and experimental studies of flow over weirs have a number of applications especially in the analyses of flow over common types of civil engineering structures. The problem of flow over weirs has been extensively studied experimentally. Most of the experimental works were performed to understand the flow characteristics of these weirs as well as the determination of the coefficients of discharge under free and submerged flow conditions (Fritz and Hager, 1998).

A review of the literature shows that little effort has so far been made to study the numerical modeling of flow over sharp crested weirs, particularly for the establishment of relationship between the discharge coefficient and the ration of the head over a weir to the weir height (C_d-h_w/t_w). The free overflow characteristics of these weirs often provide important boundary conditions for the application of large two-dimensional flow models. The significant nature of flow over such types of weirs, especially in the vicinity of flow transition from subcritical to supercritical state, is a strong departure from the hydrostatic distribution of pressure, caused by the curvatures of the streamlines. Most of the existing computational flow models, which are based on the depth-averaged Saint-Venant equations, are inappropriate to simulate this type of flow problem. In the derivation of the Saint-Venant equations, assumptions of uniform velocity and hydrostatic pressure distributions are commonly employed. Consequently, the equations represent the lowest order in approximation and cannot retain

accuracy for flow situations that involve non-hydrostatic pressure and non-uniform velocity distributions (Bhallamudi and Chaudhry, 1992). The two-dimensional nature of the flow over these weirs requires more accurate methods for exact simulation of the flow situation.

Earlier work involving flow modeling over a rectangular broad crested weir has been conducted by Hargreaves *et al.*, (2007), who investigated a weir experimentally as well as numerically via Fluent V.4.4.7. In this study, flow over sharp crested weir was highlighted. The main differences between earlier work and this research are the shape of the weir and the selection of numerical algorithms. In this paper, the commercial program Flow-3D V9.3 was used to:

- Investigate the flow patterns over a sharp-crested weir.
- Use equations to quantify the discharge over a sharp-crested weir. And
- Determine the discharge coefficient (C_d).

In the present study, results of velocity magnitude and the pressure distribution were presented to provide good basis for better understanding of the water flow over hydraulic structures.

Sharp Crested Weirs:

Classified under the term ‘sharp-crested’ or ‘thin-plate’ weirs are those overflow structures whose length of crest in the direction of flow is equal to or less than two millimeters. The weir plate should be smooth and plane, especially on the upstream face, while the crest surface and the sides of the notch should have plane surfaces which make sharp 90-degree intersections with the upstream weir face. The downstream edge of the notch should be beveled if the weir plate is thicker than two millimeters. The beveled surfaces should make an angle of not less than 45-degrees with the surface of a rectangular notch and an angle of not less than 60 degrees if the throat section is non-rectangular. Figure 1 below shows a schematic of a typical sharp-crested weir, where h_w is the head on the weir crest and t_w is the height of the weir.

In general sharp-crested weirs will be used where highly accurate discharge measurements are required, for example in hydraulic laboratories and industry. To obtain this high accuracy, provision should be made for ventilating the nappe to ensure that the pressure on the sides and surfaces of the nappe is atmospheric.

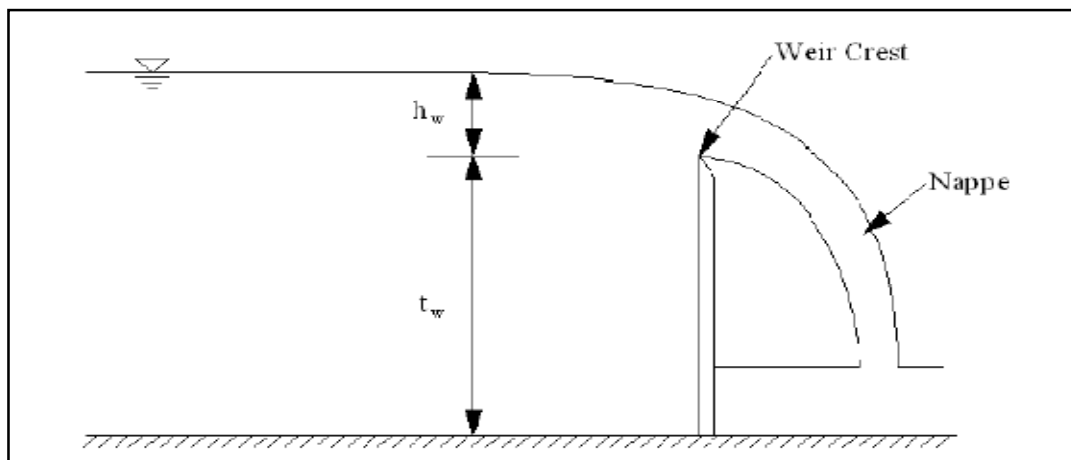


Fig. 1: Sharp-crested weir schematic.

For a sharp-crested weir, as shown in Fig. 1, the governing equation is given below according to (Rouse, 1950).

$$Q = \frac{2}{3} C_d L \sqrt{2g} h_w^{1.5} \quad (2)$$

$$H_t = \left(h_w + \frac{V^2}{2g} \right) \quad (3)$$

in which, Q is the discharge, C_d is the discharge coefficient for the weir, L is the length of the weir, H_t is the total head upstream from the weir, h_w is the piezometric head over the weir, V is the average velocity of the flow, and g is the acceleration of gravity. The equation incorporates total head (piezometric head plus velocity

head) because the velocity head affects the discharge capacity of weirs, especially those installed in shallow channels.

Rectangular Sharp-Crested Weirs:

A rectangular notch, symmetrically located in a vertical thin (metal) plate which is placed perpendicular to the sides and bottom of a straight channel, is defined as a rectangular sharp-crested weir. Rectangular sharp-crested weirs (Figure 2) comprise the following three types: a. 'Fully contracted weirs', i.e. a weir which has an approach channel whose bed and walls are sufficiently remote from the weir crest and sides for the channel boundaries to have no significant influence on the contraction of the nappe; b. 'Full width weirs', i.e. a weir which extends across the full width of the rectangular approach channel ($B/b = 1.00$) in literature, this weir is frequently referred to as a rectangular suppressed weir or Rehbock weir; and c. 'Partially contracted weir', i.e. a weir the contractions of which are not fully developed due to the proximity of the walls and/or the bottom of the approach channel.

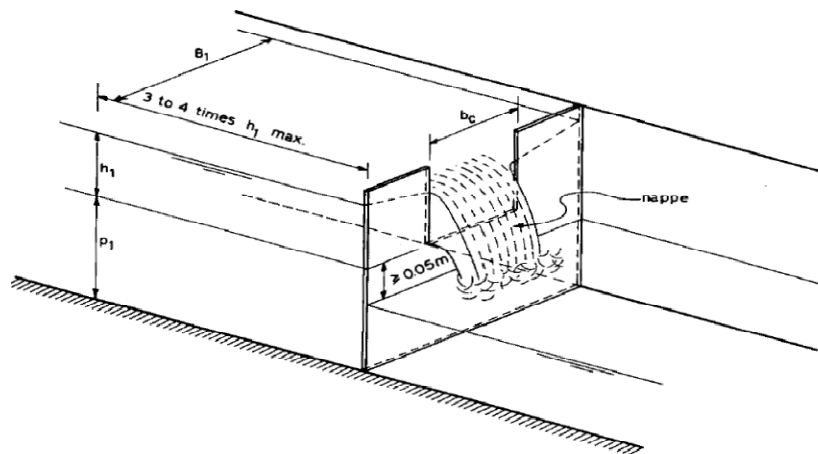


Fig. 2: Rectangular sharp-crested weir.

Numerical Model:

The CFD model used here for simulating the free surface flow over the weir was Flow-3D, developed by Flow Science in Santa Fe, New Mexico. Flow-3D is a commercial CFD package with special modules intended for hydraulic engineering applications. Despite using a structured orthogonal grid, it can model complex geometries by the application of the fractional area/volume method (FAVOR), which allows a rectangular computational cell to be partially blocked by an obstacle. The $k-\epsilon$ model is applied to the solution domain in the high Reynolds number fully turbulent flow remote from the wall. Also, The RNG method is used to eliminate the effect of small scale eddies upon the Navier-Stokes equations, by successively removing modes starting from the viscous cutoff scale. After each iteration in which a narrow band of modes is removed, the remaining modes constitute a modified system of Navier-Stokes equations, in which there is a modified effective viscosity

that becomes successively larger than the original molecular viscosity. On the other hand, the 2-D capabilities of the model were used to estimate both the velocity and pressure distribution over the weir.

Basic Theory:

The continuity and Reynolds-averaged Navier-Stokes equations are for this research solved as follows:

$$\frac{\partial u_i}{\partial x_i} = 0 \quad (4)$$

With $i = 1, 2$

$$\frac{\partial u_i}{\partial t} + U_j \frac{\partial u_i}{\partial x_j} = \frac{1}{\rho} \frac{\partial}{\partial x_j} \left\{ -p \delta_{ij} + \rho \nu_T \left(\frac{\partial u_i}{\partial x_j} + \frac{\partial u_j}{\partial x_i} \right) \right\} \quad (5)$$

Where U is the Reynolds-averaged velocity over time t , x is the spatial geometrical scale, ρ is the water density, p is the Reynolds-averaged pressure, δ is the Kronecker delta and ν_T is the turbulent eddy-viscosity. The turbulence is predicted by the standard $k-\epsilon$ model. On the other hand, the pressure is calculated according to the simple method of semi-implicit method for pressure-linked equations (Patankar, 1980).

Computation of the Free Water Surface:

Flow 3-D uses the Volume of Fluid Method (VOF). This is a two phase approach where both the water and air are modeled in the grid. The method is based on the concept that each cell has a fraction of water (F), which is 1 when the element is totally filled with water and 0 when the element is filled with air. If the value is between 1 and 0, the element contains the free water surface. Therefore, an additional transport equation is added.

$$\frac{\partial F}{\partial t} + u \frac{\partial F}{\partial x} + v \frac{\partial F}{\partial y} + w \frac{\partial F}{\partial z} = 0 \quad (6)$$

Where u and v and w are fluid velocity components in the x , y , and z directions.

Grid Generation:

The weir setup in Flow-3D was performed by inserting a STL file. In STL files solid object surfaces are approximated by triangles. AutoCAD program was used to convert the solid model into STL format. The domain was discretized using one non-uniform mesh block. The evolution in time was used as a relaxation to the final steady state. The steady state was checked through monitoring the flow kinetic energy. A grid sensitivity analysis with respect to the computational time was carried out. The grid was refined until the computational time increased disproportionately. The cell size at the beginning was 4 cm in the x -direction and was decreased to 0.50 cm. In the z -direction the size of the cells was selected to be 0.50 cm. As shown in Figure 3, a three dimensional grid with 60 cells in the x -direction, 20 cells in the y -direction, and 34 cells in the z -direction was created.

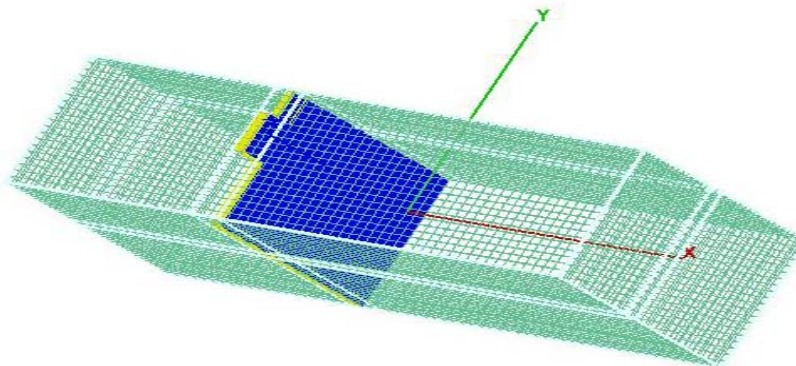


Fig. 3: 3D model grid.

Moreover, a Courant-type stability criterion is used to calculate the maximum allowed time-step size. If the Courant number is greater than 1, the velocity of a particle is so high that it passes through a cell in less than one time step. The stability criteria in Flow 3-D lead to time steps between 0.0017 and 0.002 seconds.

Boundary Conditions:

Boundary conditions for both the y and z direction was labeled as “symmetry”, which implies that identical flows occur on the other side of the boundary and hence there is no drag. In the x direction the boundary condition was “specified stagnation pressure”. With this algorithm, Flow-3D is able to model various flow heights beginning at a stagnation pressure state. A constant volume flow rate is used as inflow boundary.

A continuative boundary outflow condition, which consists of zero normal derivatives at the boundary for all quantities was used. This represented a smooth continuation of the flow through the boundary. The roughness parameter was chosen as 2 mm. Boundary conditions on the x-y-z plane are shown in Figure 4.

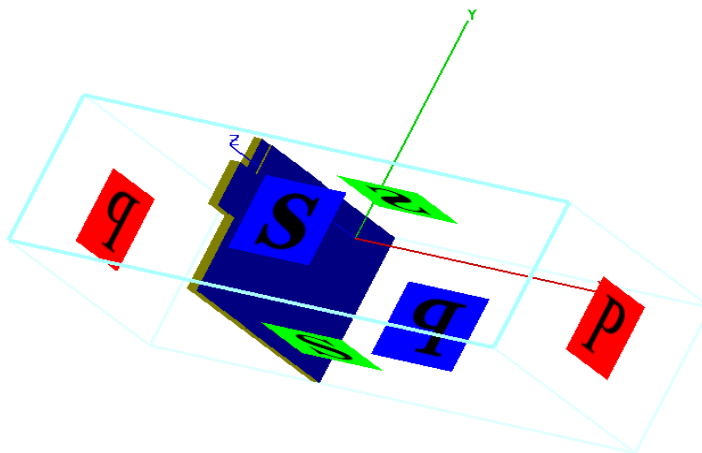


Fig. 4: Configurations of boundary conditions.

Tests:

For the purposes of this research, a solution domain of 2 m depth was chosen. The full length (5 m) of the channel was modeled. At the location of the weir, the channel is 2 m deep and 3 m wide. The weir is simply a metal plate attached to the sides of the channel.

A three-dimensional non-uniform grid was used with refinement in the near wall regions. In order to develop the free surface profile, the flow was treated as unsteady and time stepped at 0.01 s intervals until a steady state was achieved. The pressure head term in the energy equation is described below.

This form of the energy equation is normalized to the unit weight of the fluid. Therefore, the terms shown in Eq. (7) below all have dimensions of length and represent the energy head due to various forces. This form of the energy equation is also known as Bernoulli's Equation when head losses are negligible.

$$Z_1 + h_1 + \alpha_1 \frac{v_1^2}{2g} = Z_2 + h_2 + \alpha_2 \frac{v_2^2}{2g} + h_L \quad (7)$$

In Eq. (7), z is the vertical distance from a constant datum to the channel bottom, h is the water depth, v is the water velocity, α is a kinetic energy coefficient that accounts for a non-uniform flow distribution, h_L is a head loss term that occurs due to friction along the channel length and due to channel expansions or contractions between location 1 (upstream) and location 2 (downstream), and g is the gravitational acceleration constant.

Eleven different discharge rate were tested ranging from 1 m³/s to 6 m³/s. Tests were conducted for weirs with $t_w = 0.50$ m, 0.75, 1.00 m, and 1.25 m.

Results and Discussion

Tables 1-4 present the computed parameters used in estimating the value of discharge coefficient. The calculation with Flow 3-D had a grid with 114 active cells. After a computation time in the range of 435-550 seconds, a steady state condition was found. Tests with the RNG model resulted in negligible differences.

Table 1: Discharge coefficient calculations for $t_w=0.50$ m.

Q (m ³ /s)	h_w (m)	$H_t = h_w + v^2/2g$ (m)	H_w/t_w	C_d
1	0.31	0.31	0.63	0.64
1.5	0.41	0.42	0.83	0.63
2	0.49	0.50	1.00	0.63
2.5	0.57	0.58	1.17	0.63
3	0.65	0.66	1.32	0.63
3.5	0.71	0.73	1.47	0.63
4	0.77	0.80	1.60	0.63
4.5	0.85	0.88	1.75	0.62
5	0.91	0.94	1.88	0.62
5.5	0.97	1.00	2.00	0.62
6	1.01	1.05	2.1	0.62

$A = B * L$ and $B = h_w + t_w$

Table 2: Discharge coefficient calculations for $t_w=0.75$ m.

Q (m ³ /s)	h_w (m)	$H_t = h_w + v^2/2g$ (m)	H_w/t_w	C_d
1	0.31	0.31	0.41	0.64
1.5	0.41	0.42	0.56	0.63
2	0.49	0.50	0.67	0.63
2.5	0.57	0.58	0.77	0.63
3	0.65	0.66	0.88	0.63
3.5	0.71	0.73	0.97	0.63
4	0.77	0.80	1.06	0.63
4.5	0.85	0.88	1.17	0.62
5	0.91	0.94	1.25	0.62
5.5	0.97	1.00	1.33	0.62
6	1.01	1.05	1.40	0.62

Table 3: Discharge coefficient calculations for $t_w=1.00$ m.

Q (m ³ /s)	h_w (m)	$H_t = h_w + v^2/2g$ (m)	H_w/t_w	C_d
1	0.29	0.29	0.29	0.73
1.5	0.39	0.40	0.40	0.68
2	0.48	0.49	0.49	0.65
2.5	0.56	0.58	0.58	0.64
3	0.63	0.65	0.65	0.64
3.5	0.70	0.73	0.73	0.63
4	0.78	0.80	0.80	0.63
4.5	0.86	0.88	0.88	0.62
5	0.91	0.94	0.94	0.62
5.5	0.99	1.02	1.02	0.61
6	1.06	1.10	1.10	0.61

Table 4: Discharge coefficient calculations for $t_w=1.25$ m.

Q (m ³ /s)	h_w (m)	$H_t = h_w + v^2/2g$ (m)	H_w/t_w	C_d
1	0.29	0.29	0.23	0.73
1.5	0.39	0.40	0.32	0.68
2	0.48	0.49	0.40	0.65
2.5	0.56	0.58	0.46	0.64
3	0.63	0.65	0.52	0.64
3.5	0.70	0.73	0.59	0.63
4	0.78	0.80	0.64	0.63
4.5	0.86	0.88	0.70	0.62
5	0.91	0.94	0.75	0.62
5.5	0.99	1.02	0.82	0.61
6	1.06	1.10	0.88	0.61

Figure 5 shows the discharge coefficients for the sharp-crested weir plotted against H_t/t_w . Comparing the data of this study to the results of Sarginson (1972), Kindsvater and Carter (1957) and Raju and Asawa (1977) validated the data of this study for sharp-crested weirs. The comparison showed that the agreement is within $\pm 3\%$.

Examination of the data and the discharge equation revealed that the discharge coefficient is a function of the discharge. Consequently, the process to accurately obtain the discharge is iterative, requiring the simultaneous solution of the discharge equation and the relationship between H_t/t_w and the discharge coefficient as follows:

$$Q = \frac{2}{3} C_d L \sqrt{2g} \left\{ h_w + \frac{1}{2g} \left(\frac{Q}{A} \right)^2 \right\}^{\frac{3}{2}} \tag{8}$$

where A is the area perpendicular to the flow and all other variables are as previously defined.

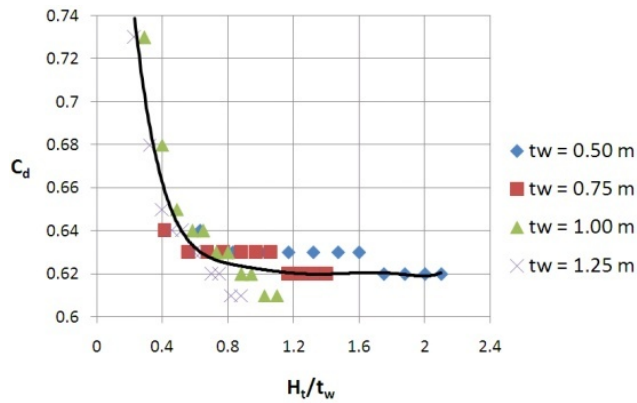


Fig. 5: Discharge coefficients for sharp-crested weirs plotted against H_t/t_w .

Figures 6-17 show the velocity vectors and the pressure distribution over the weir. The pressure proved to be hydrostatic, except for the u/s and d/s edges of the crown. As the water flows upwards over the weir, it separates from the surface of the weir at the crest and forms a nappe. The negative pressure, which could be seen in the figures can be attributed to the fact that air is trapped between the lower surface of the nappe and the downstream face of the weir. If the nappe is not fully aerated, the trapped air will create a negative pressure due to the continual aeration of the flowing water over the weir. If the water flow rate is large enough, the aeration of water will eventually remove virtually all the trapped air under the nappe.

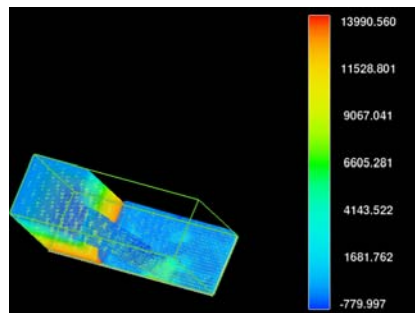


Fig. 6: 3D free surface profile ($Q = 3 \text{ m}^3/\text{s}$).

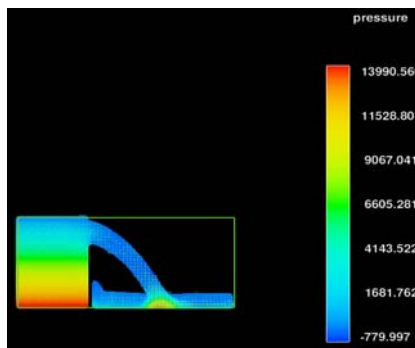


Fig. 7: 2D free surface profile ($Q = 3 \text{ m}^3/\text{s}$).

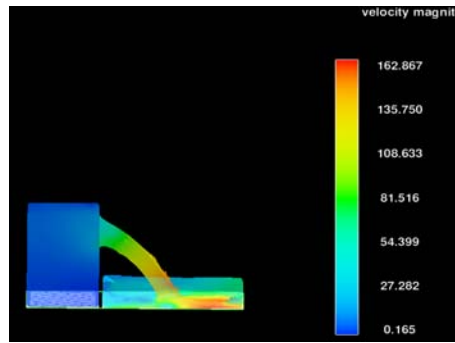


Fig. 8: 2D free surface profile ($Q = 3 \text{ m}^3/\text{s}$).

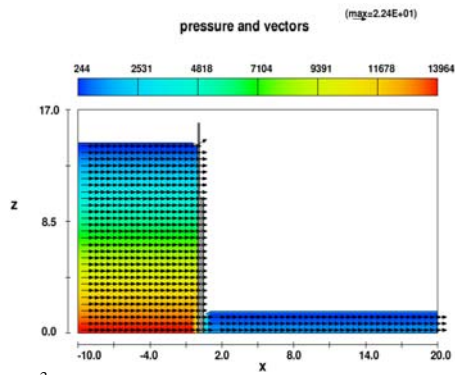


Fig. 9: Pressure distribution ($Q = 3 \text{ m}^3/\text{s}$) at $t=0.0 \text{ sec}$.

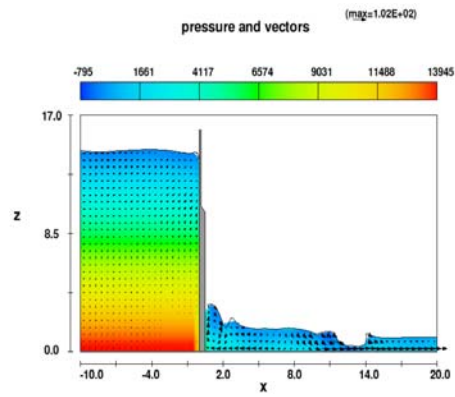


Fig. 10: Pressure distribution ($Q = 3 \text{ m}^3/\text{s}$) at $t=0.50 \text{ sec}$.

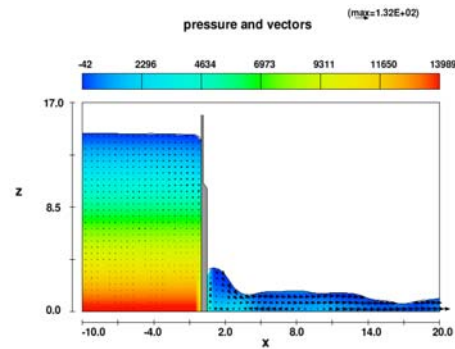


Fig. 11: Pressure distribution ($Q = 3 \text{ m}^3/\text{s}$) at $t=1.25 \text{ sec}$.

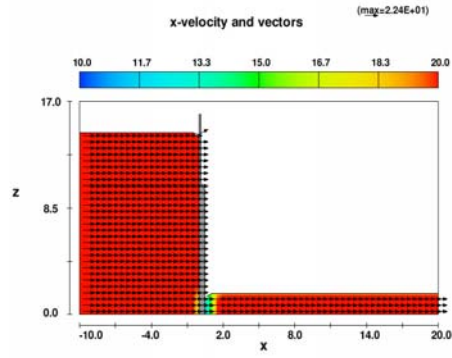


Fig. 12: X-Velocity distribution ($Q = 3 \text{ m}^3/\text{s}$) at $t=0.00 \text{ sec}$.

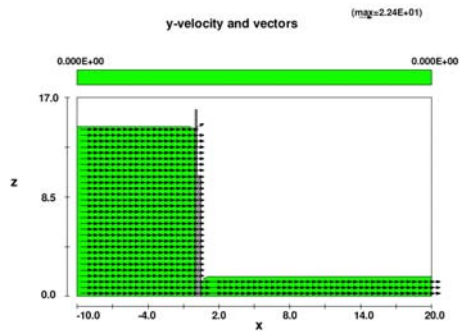


Fig. 13: Y-Velocity distribution ($Q = 3 \text{ m}^3/\text{s}$) at $t=0.00 \text{ sec}$.

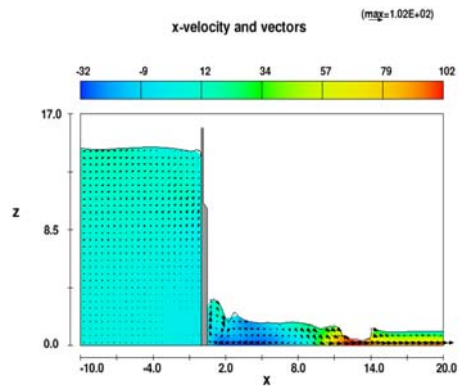


Fig. 14: X-Velocity distribution ($Q = 3 \text{ m}^3/\text{s}$) at $t=0.50 \text{ sec}$.

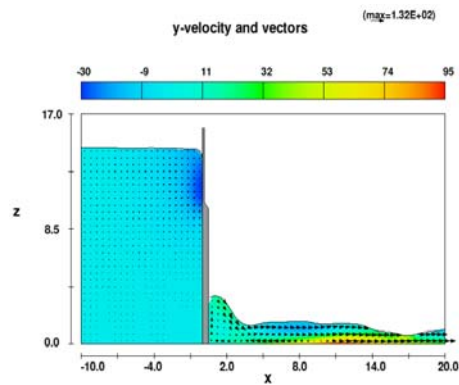


Fig. 15: Y-Velocity distribution ($Q = 3 \text{ m}^3/\text{s}$) at $t=0.50 \text{ sec}$.

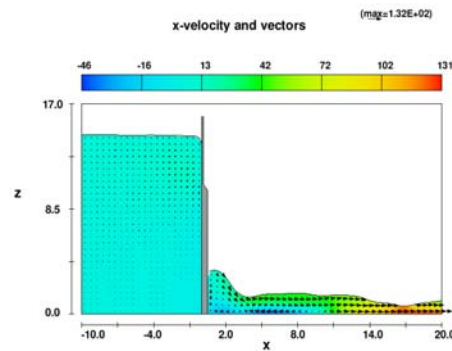


Fig. 16: X-Velocity distribution ($Q = 3 \text{ m}^3/\text{s}$) at $t = 1.25 \text{ sec}$.

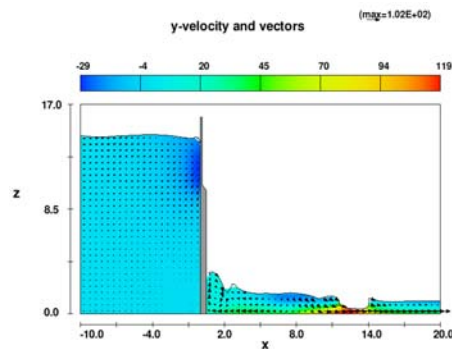


Fig. 17: Y-Velocity distribution ($Q = 3 \text{ m}^3/\text{s}$) at $t = 1.25 \text{ sec}$.

To illustrate how one would use the data, assume that a sharp-crested weir with a height (t_w) of 1 m and is installed in a rectangular channel that is 3 m wide (L). Further assume that the piezometric head (h_w), was calculated to be 1 m. The process to obtain the flow rate is as follows:

- 1) Divide h_w by t_w (because the flow and consequently the total head (H_t) are unknown, use the piezometric head (h_w) as a starting point): $h_w/t_w = 1$.
- 2) From Figure 5 obtain the C_d from the best fit C_d curve using the h_w/t_w value found in step one: $h_w/t_w = 1$, $C_d = 0.62$.
- 3) Estimate Q with Eq. 2 while neglecting the velocity head component of Eq. (3): $Q = 2/3 * 0.62 * 3 * (2 * 9.81)^{0.5} * 1^{1.5} = 5.49 \text{ m}^3/\text{s}$.
- 4) With the estimated value of Q compute the total head (H_t) by adding the piezometric head (h_w) to the velocity head (h_v): $H_t = 1 + 5.49^2 / (2 * 9.81 * 3^2 * (1 + 1)^2) = 1.04 \text{ m}$.
- 5) Compute H_t/t_w and obtain a new C_d value from Figure 5: $H_t/t_w = 1.04$, $C_d = 0.62$.
- 6) Compute a new Q with Eq. (2): $Q = 2/3 * 0.62 * 3 * (2 * 9.81)^{0.5} * 1.04^{1.5} = 5.82 \text{ m}^3/\text{s}$.
- 7) Repeat the iterative process until the estimated flow no longer appreciably changes. For this example, five iterations resulted in a flow of $5.90 \text{ m}^3/\text{s}$. The solution of Eq. (2), and the best fit curve given in Figure 5 converged on a flow $5.91 \text{ m}^3/\text{s}$. It is important to observe that simply using h_w and not H_t for this example results in the estimate of the flow being approximately 20% less than if the total head is used and the iterative solution applied. Clearly the velocity head for weirs with a shallow approach is an important factor to consider when computing the flow.

Conclusions and Recommendations:

The goal of this research was to evaluate and validate the flow over sharp-crested weirs. Flow-3D uses a high order integration to compute the movement of the water surface. Tests using flow-3D gave no differences in the results which agree with the findings of Hargreaves *et al.*, (2007). Flow 3-D was able to predict the water surface profile for the sharp crested weir and the directly linked discharge coefficient. The calculated C_d for the investigated sharp-crested weir is close to the values stated in the literature, nearly constant to 0.64. The computed C_d is hence considered to be an accurate estimate for the easily applicable discharge coefficient. Also, one of the most important advantages of using a numerical 2-3 D model is obtaining several flow parameters, such as velocity pattern and the pressure field over the whole area at the same time.

This study also showed that the important variable governing discharge over sharp-crested weirs is H_t/t_w . The use of this variable, coupled with the inclusion of the weir height in the velocity head, results in the formulation of a single curve that can be used to obtain the discharge coefficient for sharp-crested weirs rather than a family of curves. The discharge coefficient data presented can be used to accurately predict the discharge for weirs with a sharp-crest. Users of the data should be aware that the importance of the velocity head should not be neglected.

List of Symbols:

A = area (m^2)
 B = channel width (m)
 b = the length of the weir crest (m)
 C_d = discharge coefficient (-)
 g = the acceleration of gravity (m/s^2)
 H_t = the total head upstream from the weir (m)
 h_w = the piezometric head over the weir (m)
 h_L = head loss (m)
 L = the length of the weir (m)
 t_w = weir height (m)
 p = the Reynolds-averaged pressure (Pa)
 Q = discharge (m^3/s)
 U = the Reynolds-averaged velocity over time t (m/s)
 V = the average velocity of the flow (m/s)
 ν_T = the turbulent eddy-viscosity (m^2/s)
 x = the spatial geometrical scale (-)
 z = the vertical distance from a constant datum to the channel bottom (m)
 ρ = the water density (kg/m^3)
 δ = the Kronecker delta (-)
 α = a kinetic energy coefficient (-)

References

- Bhallamudi, S.M. and M.H. Chaudhry, 1994. Computation of Flows in Open Channel Transitions. *Journal of Hydraulic Research*, 30(1): 77-93.
- Fritz, H.M. and H.W. Hager, 1998. Hydraulics of Embankment Weirs. *Journal of Hydraulic Engineering, ASCE.*, 124(9): 963-971.
- Hargreaves, D.M., H.P. Morvan, N.G. Wright, 2007. Validation of the Volume of Fluid Method for Free Surface Calculation. *Engineering Applications of Computational Fluid mechanics*, 1(2): 136-147.
- Kindsvater, C.E., R.W. Carter, 1957. Discharge Characteristics of Rectangular Thin-Plate Weirs. *Journal of Hydraulic Engineering, ASCE.*, 14: 1-36.
- King, H.W. and E.F. Brater, 1963. *Handbook of Hydraulics*, 5th Edition, McGraw-Hill Book Company, New York.
- Patankar, S.V., 1980. *Numerical Heat Transfer and Fluid Flow*. McGraw-Hill Book Company, New York.
- Raju, K.G.R., G.L. Asawa, 1977. Viscosity and Surface Tension Effects on Weir Flow. *Journal of Hydraulic Engineering, ASCE.*, 103: 1227-1231.
- Rouse, H., 1950. *Engineering Hydraulics*. Proceedings of the Fourth Hydraulics Conference, Iowa Institute of Hydraulic Research, John Wiley and Sons, Inc., New York.
- Sarginson, E.J., 1972. The Influence of Surface Tension on Weir Flow. *Journal of Hydraulic Research*, 10: 431-446.